

NOTES AND CORRESPONDENCE

Assessment of Ocean Surface Winds and Tropical Cyclones around Japan by RCMs

Satoshi IIZUKA, Koji DAIRAKU

National Research Institute for Earth Science and Disaster Prevention, Tsukuba, Japan

Wataru SASAKI

Application Laboratory, Japan Agency for Marine-Earth Science and Technology, Japan

Sachiho A. ADACHI, Noriko N. ISHIZAKI

Research Institute for Global Change, Japan Agency for Marine-Earth Science and Technology, Japan

Hiroyuki KUSAKA

Center for Computational Sciences, University of Tsukuba, Tsukuba, Japan

and

Izuru TAKAYABU

Meteorological Research Institute, Tsukuba, Japan

(Manuscript received 16 July 2011, in final form 13 December 2011)

Abstract

This study assesses ocean surface winds in regional climate models (RCMs) and evaluates the ability of RCMs to downscale the features of tropical cyclones (TCs). RCMs show a smaller bias in the mean ocean surface wind around Japan during summer than the reanalysis data that is used as boundary data because of the better representation of land/ocean contrast in RCMs. However, for extreme values of ocean surface winds, all RCMs show a large bias over the ocean south of Japan.

The RCMs reasonably simulate the TC tracks for about 40% of TCs, whereas these models fail to simulate realistic TC tracks for the remaining TCs. The TC track errors in the RCMs spread over a wide range with peaks ranging from 100 to 200 km. Although two RCMs underestimate the surface wind speed associated with TCs, one RCM simulates it reasonably. Therefore, it is suggested that the bias in the extreme values of ocean surface winds can be caused not only by an insufficient representation of surface winds associated with a model TC but also by the model TC track errors. Moreover, these errors may affect the extreme values of precipitation produced by the interaction between TCs and topographies in Japan; therefore the extreme values should be used with caution. Multi-model ensemble approach contributes to reduce TC track errors. As a result, number of the TCs with the relatively small TC track errors increases up to about 60%.

Corresponding author: Satoshi Iizuka, National Research Institute for Earth Science and Disaster Prevention, 3-1 Tennodai, Tsukuba, 305-0006, Japan.
E-mail: iizuka@bosai.go.jp
© 2012, Meteorological Society of Japan

1. Introduction

There has been an increasing public concern about climate changes, and hence, regional assess-

ment of climate change impacts has become a pressing issue for many countries. Since regional climate behavior is influenced not only by the global climate but also influenced by local terrain and land use, global climate models, which have coarse resolution, cannot provide high-resolution information for use in the assessment of water resources, agriculture, and vulnerability around coastal oceans. Therefore, statistical downscaling or dynamical downscaling using high-resolution regional climate models (RCMs) is required to downscale outputs of global climate model to the regional or local scale.

Intense wind and heavy precipitation associated with tropical cyclones (TCs) occasionally cause severe damages in Japan. A statistical approach is often used for a TC wind assessment using synthetic storm tracks with a parametric model (e.g. Hallegatte 2007). However, such models may be not suitable for TCs moving into mid-latitude because of synoptic interactions that lead to extratropical transition. Furthermore, these models cannot simulate precipitation associated with TCs. Therefore, it is expected that RCM simulations will reproduce the correct intense wind and precipitation values associated with TCs.

The dynamical downscaling technique should retain the large-scale features of a global reanalysis data or global models and add information on smaller scales. However, it can be expected that an RCM exhibits certain level of internal variability due to nonlinearities in the model's physics and dynamics; this variability can modulate physically forced signals in the model. Thus, it is important to evaluate the internal variability of an RCM. Alexandru et al. (2007) showed that strong precipitation events can cause the internal variability in RCMs, and the associated internal variability continues to develop along the downwind side of the domain. Giorgi and Bi (2000) analyzed the sensitivity of an RCM to initial and boundary conditions over eastern Asia. The results showed that the internal variability of the RCM was insensitive to the amplitude of perturbations in the initial conditions. They also found that the internal variability exhibited a pronounced summer maximum. This is because the internal model variability, related to factors such as random and nonlinear behavior in convection and precipitation processes and associated local land-atmosphere interactions, is at a maximum in the summer, and a stronger westerly flow in the winter sweeps away the internally generated model response.

Uncertainties of TCs simulated in RCMs have been examined in several studies. The recent study for the dynamically downscaled TC activity has succeeded in improving the TC intensity simulated in RCMs as a result of an increase in the resolution (Bender et al. 2010). Wu et al. (2011) examined the sensitivity of TC frequency to the initial conditions. On the other hand, Landman et al. (2005) showed that the model TC track is sensitive to the choice of RCM domain. Feser and von Storch (2008) and Liu and Xie (2011) showed that the spectral nudging technique can reduce TC track error simulated in RCMs. However, it is not well examined how much uncertainty exists in TC tracks around Japan simulated by RCMs. An assessment of the ability of RCMs to reproduce correct tracks and intensities of TCs would help to understand the uncertainties in the downscaled information on climate changes. In Japan, as part of a large collaborative project (S-5-3), long-term RCM simulations were performed to provide climate change information on a regional or local scale (Takayabu 2010). In these simulations, all RCMs have the same resolution and use the same data as boundary conditions. This project enables us to evaluate the ability of RCMs to dynamically downscale the features of TCs. This paper is organized as follows: section 2 briefly describes the RCMs used in this study. The results are presented in section 3, and the conclusion is given in section 4.

2. Model and data

In this study, we compared the features of ocean surface winds and TCs, which were downscaled using the following three RCMs: a non-hydrostatic regional model (NHM) based on the operational model in the Japan Meteorological Agency (JMA) (Saito et al. 2006), an advanced research version of the weather research and forecasting model (WRF) (Skamarock et al. 2005), and a regional atmospheric modeling system (RAMS) (Pielke et al. 1992). The hourly sea level pressure, surface wind at 10 m, and accumulated precipitation of the NHM, WRF, and RAMS are provided by the Meteorological Research Institute, University of Tsukuba, and the National Research Institute for Earth Science and Disaster Prevention, respectively. The configurations of the RCMs are presented in Table 1. All the models covered the whole of Japan with a same grid interval of 20 km, although the model domain sizes varied slightly from one model to another (Fig. 1). The topography and

Table 1. Summary of configurations of RCMs used in the present study.

	NHM	WRF	RAMS
Horizontal resolution	20 km	20 km	20 km
Grids (longitude \times latitude \times vertical)	171 \times 161 \times 40	129 \times 139 \times 31	128 \times 144 \times 27
Map projection (Center pole)	Lambert (140°E, 30°N)	Polar stereo (137.5°E, 36°N)	Rotated Polar (137.5°E, 36°N)
Dynamic process	Nonhydrostatic	Nonhydrostatic	Nonhydrostatic
Grid points in buffer zone	20 grids	5 grids	5 grids
Cumulus parameterization	Kain and Fritsch	Kain and Fritsch	Kain and Fritsch
Cloud Microphysics	Three-ice bulk microphysics scheme	WSM 6-class scheme	Scheme proposed by Walko et al.
Planetary boundary layer	Mellor-Yamada level 3	Mellor-Yamada Nakanishi-Niino level 2.5	Mellor-Yamada level 2.5
Land surface	Simple Biosphere model	NOAH land surface model	LEAF2 + GEMTM
Time integration	1-year slice (14 months)	1-year slice (14 months)	Sequential
Initial time	July 1 each year	November 1 each year	January 1, 1979
Spin-up time	2-months (July–August) each year	2-months (November–December) each year	

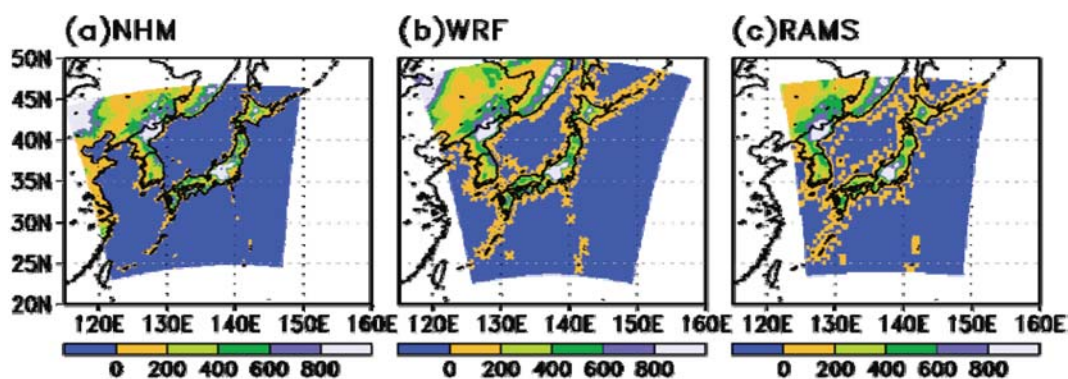


Fig. 1. Topographic height (m) in the computational domain of NHM (a), WRF (b), and RAMS (c).

land-sea distributions also differed slightly among the RCMs as a result of different grid projections and smoothing methods of topography, though the same topographic data is commonly used. These models were simulated for the 20-year period from 1985 to 2004, using the data of the Japanese long-term Re-analysis project (JRA) (Onogi et al. 2007) as boundary conditions. A more detailed description of the RCMs is provided in Iizumi et al. (2011).

Many numerical studies for TC activities use the automatic algorithm to detect and track model TCs, and it is pointed out that the frequency of model TCs is sensitive to the criteria used in the tracking algorithm (e.g. Wu et al. 2011). However, such methods were not used in the present study. We first selected a TC that was observed in a range of longitudes from 126°E to 146°E and latitudes from 25°N to 46°N for at least more than a day. This TC was selected from the best track data com-

piled by the Regional Specialized Meteorological Center (RSMC)–Tokyo Typhoon Center of the JMA. The RSMC best track data include the locations, central pressure, and radius of 15 m s^{-1} wind speed (R15) of TCs at successive 6-hour intervals. The region of analysis covered by all three RCMs was selected. We then guessed model TC positions using the following definitions:

1. The grid point with minimum sea level pressure in a 15×15 grid-point box is defined as the center of a TC, and
2. The difference in the sea level pressure between the center of the TC and each grid point on the boundaries that is less than 25 grid points away from the center is greater than 1 hPa.

The TC tracks in the JRA data were also identified using similar definitions. Then, the model TC positions were selected from the guessed grid points with the sea level pressure minimum around the observed TC positions based on the best track data. Note that the TCs that are independently generated in the RCMs are not detected in the present analysis. After identifying the model TC tracks using the above methods, we finally modified the obtained model TC tracks by hand through comparisons with the surrounding sea level pressure fields, because some model TCs sometimes take the different tracks from observed ones. For the period 1985–2004, a total of 202 TCs passed around Japan, but 10 of which were not simulated in any RCM (Table 2) and hence not used in this study. Consequently, we assess 192 TCs in the present study. Note that a few TCs are not identified even in the JRA data because the best track data used in the assimilation system of the JRA data is different from the RSMC best track data (Hatsushika et al. 2006).

To validate the simulated ocean surface winds and the structure of model TCs, we used the 6-hourly Blended Sea Winds (BSW) which combined the satellite-measured ocean surface winds with the atmospheric model winds (Zhang et al. 2006) and is provided by the National Oceanic and Atmospheric Administration/National Climate Data Center. The spatial grid resolution is 0.25° .

3. Results

We first show the climatology of the mean and 99th-percentiles of the satellite-based ocean surface winds during summer (July–September), and the root mean square error (rmse) of the ocean surface winds obtained by comparing BSW and the data

Table 2. A list of selected TC number IDs used in the present study. A TC number ID not detected in the RCMs is under-lined.

Year	Tropical Cyclone Number ID
1985	03, 06, 07, 08, 09, 10, 12, 13, 14, 20, 24
1986	06, 08, 10, 13, 15, 16, 17, 18
1987	04, 05, 07, <u>08</u> , <u>10</u> , 12, 13, 16, 19
1988	04, 07, 08, 11, <u>13</u> , <u>15</u> , 16, 18, 24, 26
1989	06, 11, 12, 13, 14, 17, 21, 22, 25, 28
1990	07, 10, 11, 14, <u>15</u> , 19, 20, 21, 28
1991	09, 10, 12, <u>13</u> , 14, 15, 17, 18, 19, 21, 23
1992	03, 09, 10, 11, 14, 16, 17, 19, 22, 28, 30
1993	04, 05, 06, 07, 11, 13, 14, 19, 20, 21
1994	07, 11, 14, <u>16</u> , 21, 26, 29, 31, 34
1995	02, 03, 07, 12, 13, 14, 17, 18
1996	03, 04, 05, 06, 12, 14, 17, 20, 21, 24
1997	04, 06, 07, 08, 09, 11, 13, 18, 19, 20, 23, 24
1998	04, 05, 06, 07, <u>08</u> , 09, 10, 11
1999	04, 05, 07, 08, 09, 10, 13, <u>16</u> , 17, 18
2000	02, 03, 05, 06, 08, 09, 12, 14, 17, 19
2001	01, 02, 06, 09, 11, 15, 16, 17, 20, 21
2002	04, 05, 06, 07, 08, 09, 11, 13, 15, 16, 19, 21
2003	04, 05, 06, 10, 14, 15, 16, 17, 21
2004	02, 04, 06, 07, 08, 10, 11, 15, 16, 18, <u>19</u> , 21, 22, 23, 24

of JRA, NHM, WRF, and RAMS (Fig. 2). The 99th-percentiles are presented as a relatively robust measure for extreme winds. On average, the ocean surface wind speed around Japan is calm during summer (Fig. 2a). This feature is well simulated in all RCMs as well as the JRA data (Figs. 2b–e). However, a notable bias is observed in the ocean surface wind speed around the coastal area for the JRA data because of the insufficient representation of land/ocean contrast due to the coarse horizontal resolution (Fig. 2b). High-resolution RCMs are successful in reducing this bias, although the bias is still found in the vicinity of the Japanese islands. However, it should be noted that the accuracy of the ocean surface wind speed measured by microwave remote sensors close to a coast is limited

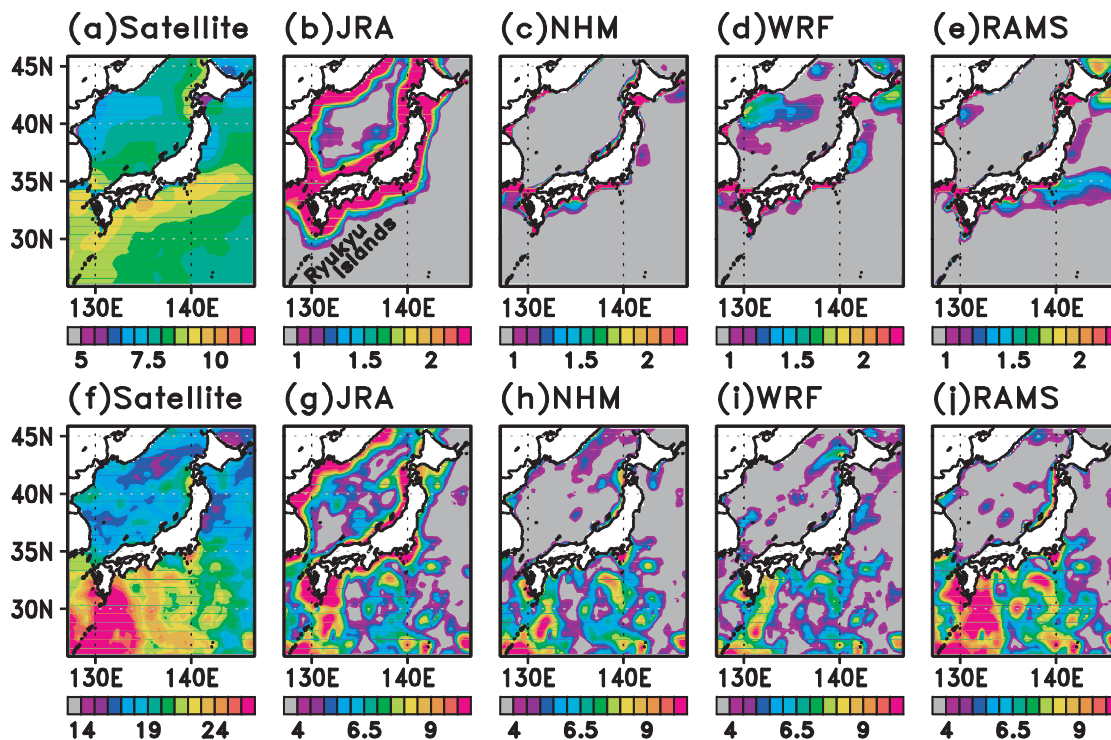


Fig. 2. Mean of the ocean surface wind speed for summer (July–September) in the BSW estimated during the period 1999–2004 (a). The rmse of the ocean surface wind speed between the BSW and JRA (b), NHM (c), WRF (d), and RAMS (e). Unit is m s^{-1} . Same as in (a)–(e) but for the 99th percentiles (f)–(j). The location of the Ryukyu Islands is denoted in (b).

(Pickett et al. 2003). The capabilities of RCMs to reduce the wind speed bias in coastal regions are also reported in several studies (e.g. Winterfeldt and Weisse 2009).

While the RCMs simulate the average ocean surface wind speed well, they show a remarkable bias in the extreme surface wind speed over the ocean south of Japan, particularly, around the Ryukyu Islands (Fig. 2f–j). Because TCs can cause intense surface wind speeds around Japan during summer, these biases in the ocean surface wind speed may be one of the reasons for problems in the representation of model TCs.

Figure 3 shows the relationship between TC central pressure of the JRA data and the best track data and that of the three RCMs. The central pressure of all the TCs in the JRA data is underestimated, although the prominent feature of the JRA data is its embedded idealized TC structure (Hatsushika et al. 2006). One possible reason for this discrepancy is the relatively coarse resolution of the model used in the assimilation system of the

JRA data. Although the RCMs simulated more intense TCs compared with the JRA data, the central pressure of the simulated TCs in the three RCMs still overestimates compared with the central pressure of the best track data. These biases in the RCMs suggest that the horizontal resolution of the RCMs is not enough to reproduce the central pressure of TCs as observed.

Other measures of TC intensity are surface winds. Thus, we compared the profiles of the surface wind associated with the model TCs with the observations. Because the satellite-measured surface wind has been available since 1999, we compared the 99th percentiles of the surface wind speed of TCs observed from 1999 to 2004. The surface wind speed associated with TCs is well simulated in WRF while the other two RCMs underestimate the surface wind speed associated with TCs (Fig. 4). This suggests that the surface wind speed associated with TCs in RCMs is sensitive not only to the horizontal resolution but also to the difference in physical processes. However, it should be noted

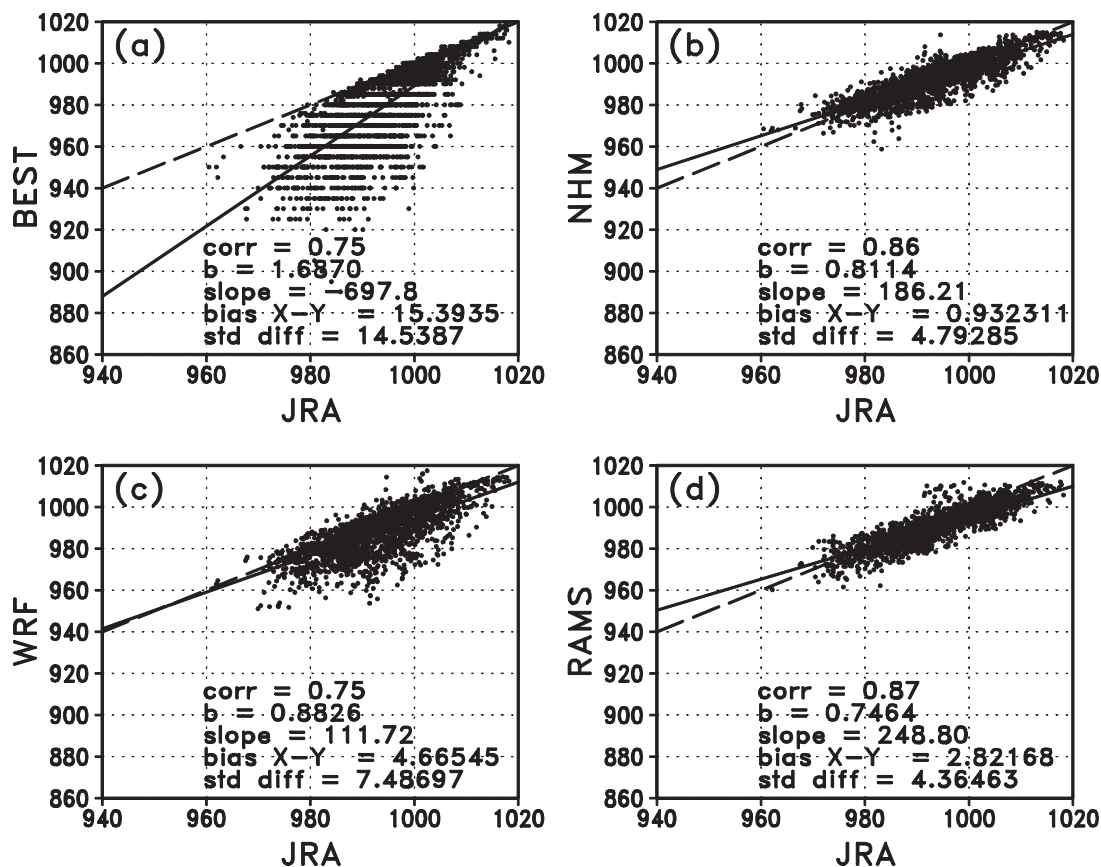


Fig. 3. Scatter diagrams for the central sea level pressure of the TC for best track data (a), NHM (b), WRF (c), and RAMS (d) against that for the JRA data. Unit is hPa. Linear regression lines are shown by solid lines and 1:1 lines are shown by dashed lines.

that the surface wind associated with TCs simulated by WRF may be unrealistic because the sea level pressure of the simulated TCs is still overestimated compared with the central pressure of the best track data (Fig. 3c).

Reproducing the correct TC tracks is also an important issue for the use of climate change information that is downscaled to a regional or local scale. This is because TCs sometimes cause heavy rainfall due to the interaction with complex topography and intense winds over Japan, and so TC track errors can cause bias in such the fields in RCMs. Figure 5 shows the geographic distributions of TC track errors simulated in the RCMs. The remarkable accumulation of the model TC track errors is observed over the regions where there are the large biased of the 99th-percentiles of the simulated surface winds (Fig. 2). This suggests that the bias in the extreme values of ocean

surface winds may be caused not only by an insufficient representation of surface winds associated with a model TC but also by the model TC track errors.

We assessed TC track errors for 192 cases for which all three RCMs are available. The TC track errors in the RCMs spread over a wide range with peaks from 100 to 200 km (Fig. 6a). However, considering the average lifetime of a selected TC (~ 2.5 days), the TC track errors are within the range of values obtained over 60 h using the operational TC forecast models (Goerss 2000; Kumar et al. 2003). Among the three RCMs, WRF has the highest accuracy in simulating TC tracks, which may be related to the degree of representation of surface wind associated with TCs (Fig. 4). This is partially because the model TC track errors result from mishandling the interaction of the circulation of the TC itself with adjacent environmental circu-

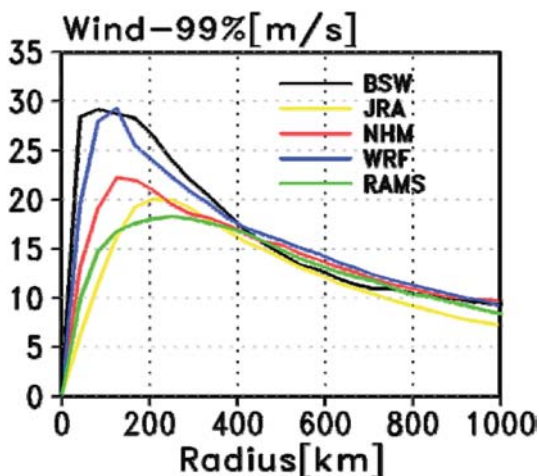


Fig. 4. Profile of the 99th percentiles of the ocean surface wind speed of a TC as a function of radial distance from the center (a). Unit is m s^{-1} . Black line indicates the 99th percentiles estimated from the BSW. The corresponding values for JRA, NHM, WRF, and RAMS are shown as yellow, red, blue, and green lines, respectively. The 99th percentiles are estimated from TCs observed during the period 1999–2004 after satellite data became available.

lations involving mid-latitude circulation and subtropical anticyclonic circulation (Carr and Elsberry 2000a, b). However, it should be noted that other RCMs occasionally have a higher accuracy in sim-

ulating TC tracks than WRF. As a result, a simple ensemble mean of the TC track generally shows a smaller rmse of TC tracks than those shown by individual RCMs (Fig. 6a).

When considering the profile of the surface wind speed associated with TCs (Fig. 4), it is expected that about 200 km of the model TC track error can cause about 10 m s^{-1} of the surface wind speed bias observed in 99th-percentiles of the ocean surface winds during summer in the WRF model (Fig. 2). This suggests that the bias in extreme ocean surface wind speed can be caused not only by the insufficient representation of surface winds associated with model TCs but also by the track errors of the model TCs. Furthermore, the results imply that the RCMs have limited ability in terms of adding information about the precipitation, produced by the interaction between TCs and complex small-scale topographies through the TC track errors, as well as its insufficient precipitation intensity.

To examine the similarity of TC tracks among the RCMs, the spread of TC track errors against the ensemble mean TC track errors among the RCMs is presented in Fig. 6b. The TC track errors of the RCMs can be classified into four clusters (Elsberry and Carr 2000): small ensemble error and small spread (SESS), small ensemble error and large spread (SELS), large ensemble error and small spread (LESS), and large ensemble error and large spread (LELS). An example of TC tracks for each category is shown in Fig. 7.

There is no clear correlation between the en-

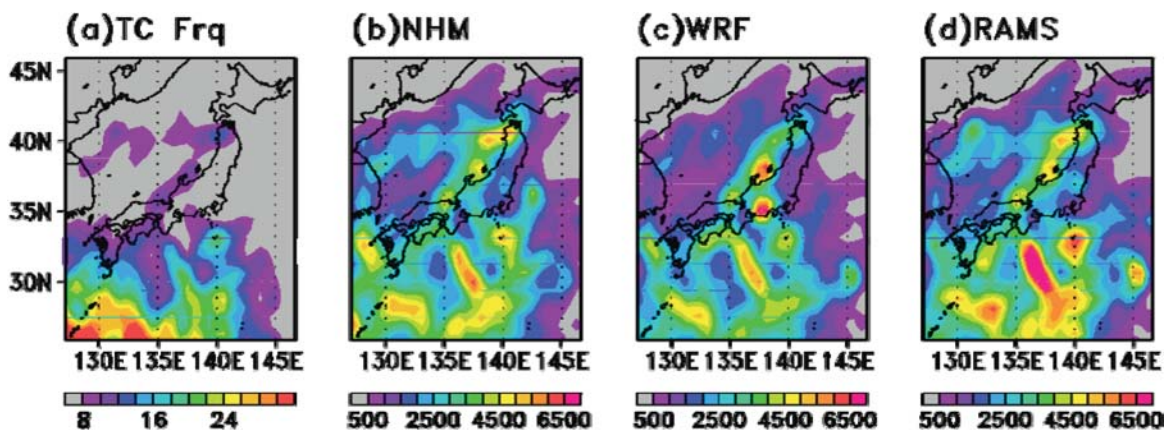


Fig. 5. (a) Geographic distribution of TC occurrence during the period 1985–2004. (b) Geographic distribution of accumulated TC track error during the period 1985–2004 for NHM. Unit is km. (c) Same as in (b) but for WRF. (d) Same as in (b) but for RAMS. The density is obtained by counting the number of TC occurrence (model TC track error to JRA track) in each $0.625^\circ \times 0.625^\circ$ latitude–longitude grid box.

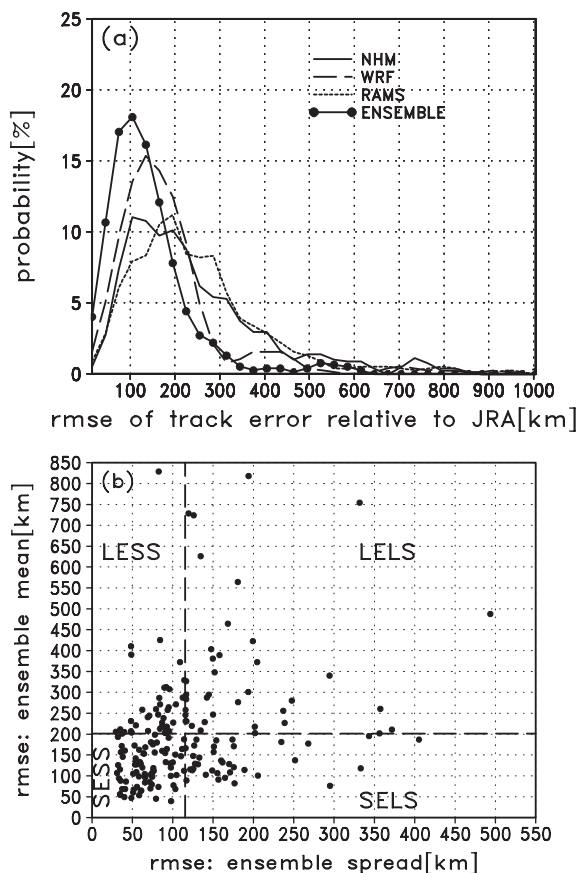


Fig. 6. Probabilities of rmse in each TC track simulated in the three RCMs relative to the TC track in JRA (a). Scatter diagrams for rmse in each TC track between the ensemble mean of the three RCMs and the JRA, against the ensemble spread among the RCMs (b). Unit is km. Averaged values of the rmse of the ensemble mean and the spread are shown as a dashed line.

semble mean rmse and the spread, and the average of the ensemble mean rmse is approximately twice that of the ensemble spread (Fig. 6b). This is similar to the results based on operational models (Goerss 2000; Elsberry and Carr 2000). When we define the average of the ensemble mean rmse (201 km) and the average of the spread (115 km) as the criterion for dividing individual categories, 40% of the TCs are classified into the SESS category, whereas about 20% of the TCs are classified respectively into the other categories. Multi-model ensemble superiority is caused not only by error

compensation but also by its greater consistency and reliability (Hagedorn et al. 2005). In this study, the merit of the multi-model ensemble approach to reduce TC track errors is found for about 60% of the TCs classified into the SESS and SELS categories. However, even using the multi-model ensemble approach, the RCMs fail to simulate the realistic tracks for the remaining TCs classified into the LESS and LELS categories.

Figure 8 shows the percentage of each category for TC of large, medium, and small size, respectively. Here, we used the radius of 15 m s^{-1} wind speed (R15) included in the best track data to determine the size of TCs. The R15 averaged during the period when a TC moves over the analysis domain was computed to estimate the typical size of each TC size. Then, the TCs were categorized as large, medium, and small size, respectively, using 500 km and 300 km as the criteria. It is found that the percentage of the SESS category TC becomes larger, as the TC size is larger. This suggests that the degree to represent TC in the boundary data generally contributes to reduce TC track errors in RCMs. However, there are some LESS category TCs (TY8713, 8917, 9021, 9028, 9121, 9320, 9512, 9621, and 0423) despite the large TC size. Since three of them (TY9021, TY9512, and TY0423) have the relatively smaller cross-track errors than the others (Figs. 9c, 9g, and 9i), their large track errors result mainly from the along-track errors. Carr and Elsberry (2000b) describe that the response to vertical shear (RVS) process tends to decrease the intensity of the model TC, which usually results in a decrease in translation speed as the TC then responds to a slower environmental steering over a shallower layer. In other words, the bias in the model TC intensity can be responsible for the TC track error. On the other hand, the remaining LESS category TCs have the relative larger systematic cross-track errors, and four of them are binary TCs (TY8713, 9121, 9320, and 9621). It seems that the counterpart of the binary TC causes the change in the translation direction of TCs accompanied by the slow bias of the model TC. The cross-track error in TY9028 (Fig. 9d) seems to be caused by the midlatitude synoptic low pressure on the western side of the TC. Even though the counterpart of the binary TC exists outside the model domain, the bias seems to be caused through boundary forcing (Figs. 9a and e). Note that the bias in TY9621 seems to result rather from mishandling the interaction of the circulation of the simulated TC itself

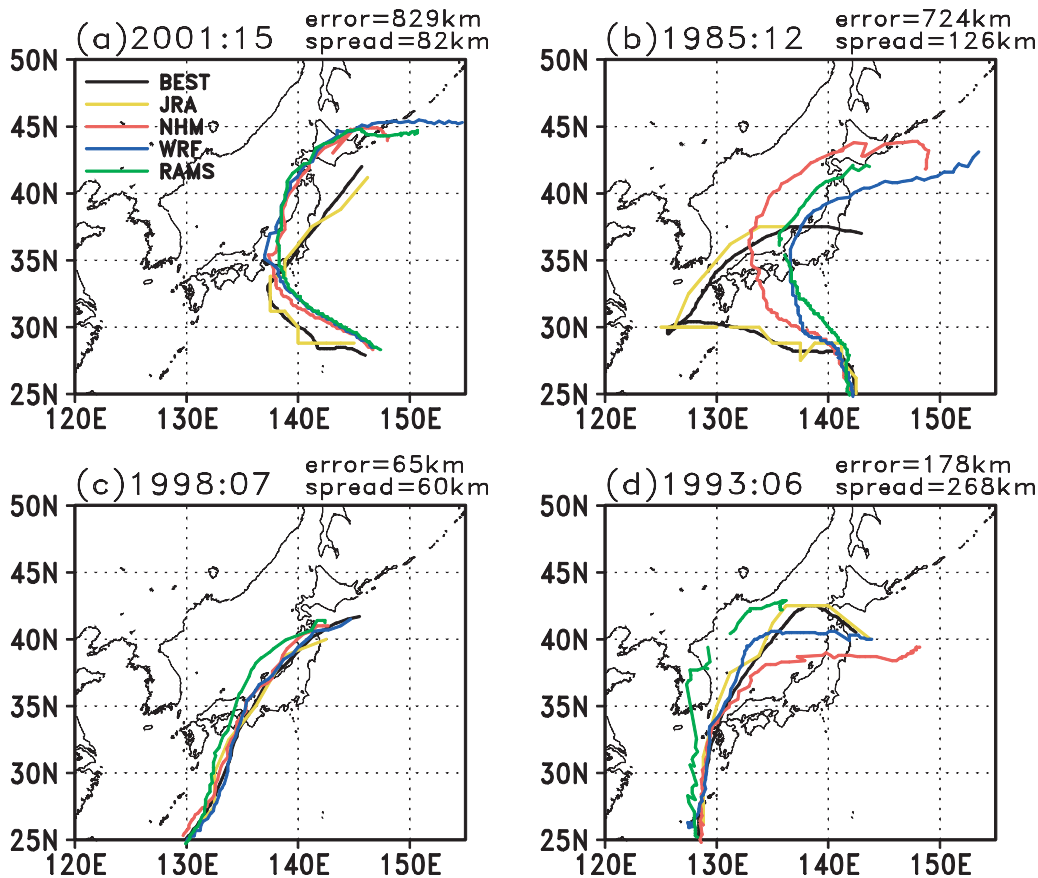


Fig. 7. Tracks of TY0115 (a), TY8512 (b), TY9807 (c), and TY0306 (d) as an example of the LESS, LELS, SESS, and SELS categories, respectively. Tracks of best track data, JRA, NHM, WRF, and RAMS are shown as black, yellow, red, blue, and green lines, respectively. The ensemble mean error and the spread of each TC track are indicated on the top of the panels.

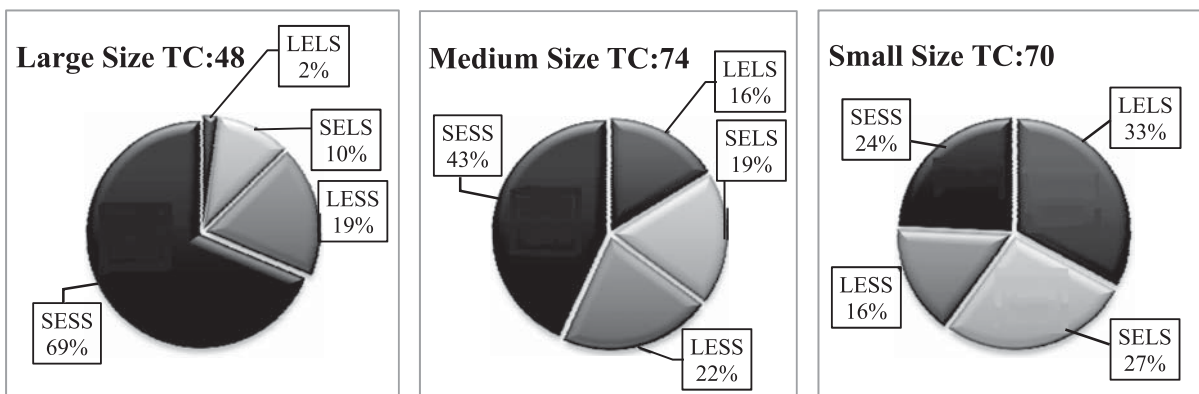


Fig. 8. Percentage of each category for TC of large (left panel), medium (center panel), and small size (right panel), respectively. Radius of 15 m s^{-1} wind speed (R15) averaged during the period when a TC moves over the analysis domain are used to define each TC size. Using 500 km and 300 km as the criteria, the TCs are categorized as large, medium, and small size. Number of each TC size is shown on top of each panel.

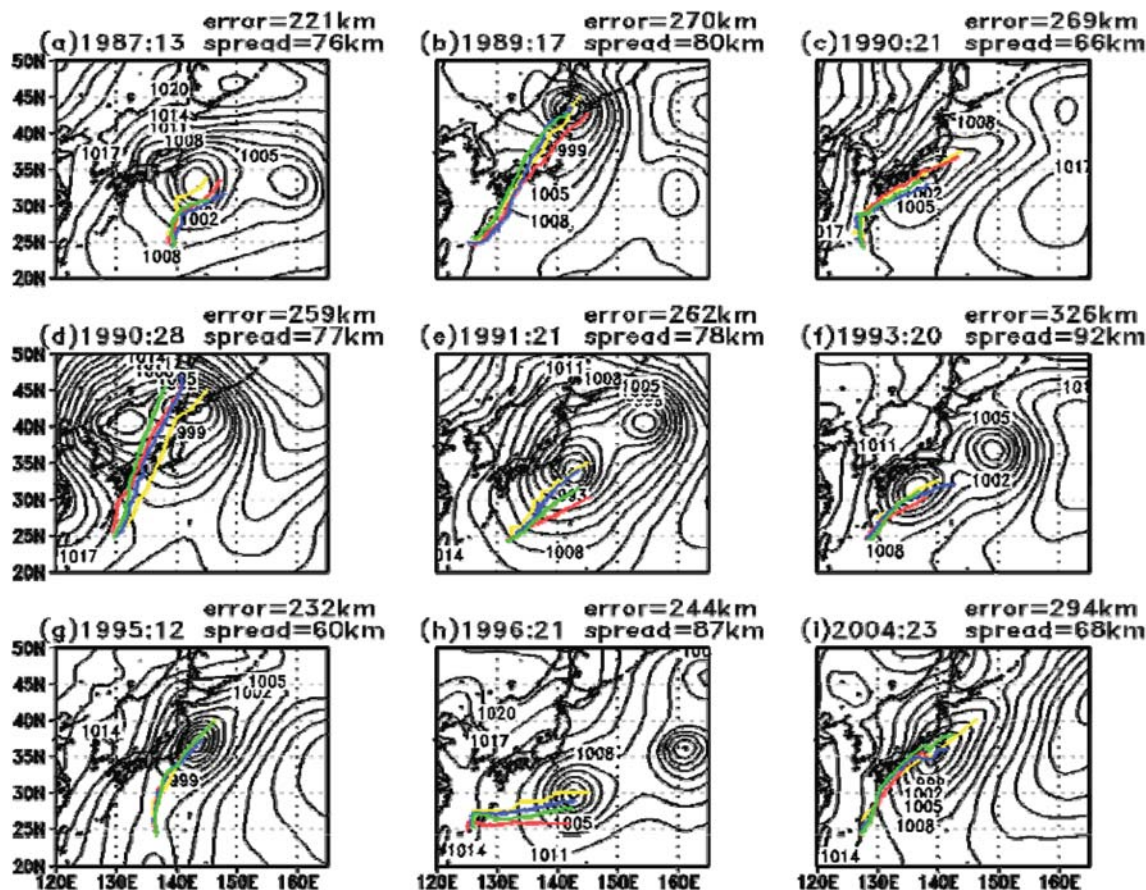


Fig. 9. Tracks of the LESS category TC with large size. TY8713 (a), TY917 (b), TY9021 (c), TY9028 (d), TY9121 (e), TY9320 (f), TY9512 (g), TY9621 (h), and TY0423 (i). Tracks of JRA, NHM, WRF, and RAMS are shown as yellow, red, blue, and green lines, respectively. The ensemble mean error and the spread of each TC track are indicated on the top of the panels. Sea level pressure of JRA is also shown by contours. Contour interval is 3 hPa.

with the circulations induced by the same TC of the boundary data (Fig. 9h), because the TC moves near the southern boundary of the model domains (Fig. 1). Thus, it is suggested that the small domain size occasionally can cause large TC track errors. On the other hand, it is difficult to identify the reasons causing the large spread of model TC track error from the comparison in the present study, because the various differences in configurations of the RCMs can cause the spread. The further analysis of TCs in RCMs incorporated with a spectral nudging technique for dynamical downscaling (Kida et al. 1991; von Storch et al. 2000) technique and also sensitivity experiments in future would help to understand the internal variability in RCMs.

4. Summary

In this study, we assessed the ocean surface winds in RCMs and evaluated the ability of RCMs to downscale the features of TCs. All three RCMs used in this study have the same resolution and use the same data as boundary conditions. The RCMs showed a smaller bias in the mean ocean surface wind around Japan during summer than the reanalysis data that is used as boundary conditions, because of the better representation of land/ocean contrast in RCMs. However, for extreme values, all the RCMs showed a large bias over the ocean south of Japan.

The comparison of model TCs among the RCMs shows that one RCM simulated the surface wind

speed associated with TCs reasonably well, unlike the other two RCMs that underestimated it. However, none of these models simulates realistic TC tracks for about 40% of TCs. Therefore, it is suggested that the bias in extreme ocean surface winds can be caused not only by an insufficient representation of surface winds associated with model TCs but also by the model TC track errors. On the other hand, the TC tracks for about 40% of TCs are reasonably simulated in all the RCMs. In addition, it is found that a multi-model ensemble approach contributes to reduce TC track errors. As a result, number of the TCs with the relatively small TC track errors increases up to about 60%. This suggests that a multi-model ensemble approach may produce more accurate TC tracks, on average, than the individual model. Furthermore, it is found that the TC track errors generally become smaller, as the TC size is larger. This suggests that the degree to represent TC in the boundary data contributes to reduce TC track errors in RCMs.

Although an improvement of models may reduce the absolute bias in TC track and intensity, the relative portion of TC track errors in RCMs would remain through various factors. Thus, the internal variability related to TCs is inherent to RCMs. However, it is certainly necessary to reduce the systematic model bias of TC track and intensity in RCMs to provide the better climate information.

Acknowledgments

This research was supported by the Global Environment Research Project Fund (S-5-3) of the Ministry of the Environment, Japan, and partially supported by the Research Project under the National Research Institute for Earth Science and Disaster Prevention, the Research Project “Hot Spot of Midlatitude Air–Sea Interaction”, and grants-in-aid (22310111) from the Japanese Ministry of Education, Culture, Sports, Science, and Technology. We thank two anonymous reviewers for their comments, which greatly improved the original version of this paper.

References

- Alexandru, A., R. D. Elia, and R. Laorise, 2007: Internal variability in regional climate downscaling at the seasonal scale. *Mon. Wea. Rev.*, **135**, 3221–3238.
- Bender, M., T. R. Knutson, R. E. Tuleya, J. J. Sirutis, G. A. Vecchi, S. T. Garner, and I. M. Held, 2010: Modeled impact of anthropogenic warming on the frequency of intense Atlantic hurricanes. *Science*, **327**, 454–458.
- Carr, L. E., III, and R. L. Elsberry, 2000a: Dynamical tropical cyclone track forecast errors. Part I: Tropical region error sources. *Wea. Forecasting*, **15**, 641–661.
- Carr, L. E., III, and R. L. Elsberry, 2000b: Dynamical tropical cyclone track forecast errors. Part II: Mid-latitude circulation influences. *Wea. Forecasting*, **15**, 662–681.
- Elsberry, R. L., and L. E. Carr III, 2000: Consensus of dynamical tropical cyclone track forecasts—errors versus spread. *Mon. Wea. Rev.*, **128**, 4131–4138.
- Feser, F., and H. von Storch, 2008: A dynamical downscaling case study for Typhoons in Southeast Asia using a regional climate model. *Mon. Wea. Rev.*, **136**, 1806–1815.
- Giorgi, F., and X. Bi, 2000: A study of internal variability of a regional climate model. *J. Geophys. Res.*, **105**, 29,503–29,521.
- Goerss, J. S., 2000: Tropical cyclone track forecasts using an ensemble of dynamical models. *Mon. Wea. Rev.*, **128**, 1187–1193.
- Hagedorn, R., F. J. Doblas-Reyes, and T. N. Palmer, 2005: The rationale behind the success of multi-model ensembles in seasonal forecasting—I. Basic concept. *Tellus*, **57A**, 219–233.
- Hallegatte, S., 2007: The use of synthetic hurricane tracks in risk analysis and climate change damage assessment. *J. Appl. Meteor. Clim.*, **46**, 1956–1966.
- Hatsushika, H., J. Tsutsui, M. Fiorino, and K. Onogi, 2006: Impact of wind profile retrievals on the analysis of tropical cyclones in the JRA-25 reanalysis. *J. Meteor. Soc. Japan*, **84**, 891–905.
- Iizumi, T., M. Nishimori, K. Dairaku, S. A. Adachi, and M. Yokozawa, 2011: Evaluation and intercomparison of downscaled daily precipitation indices over Japan in present-day climate: Strengths and weaknesses of dynamical and bias correction-type statistical downscaling methods. *J. Geophys. Res.*, **116**, doi:10.1029/2010JD014513.
- Kida, H., T. Koide, H. Sasaki, and M. Chiba, 1991: A new approach to coupling a limited area model with a GCM for regional climate simulation. *J. Meteor. Soc. Japan*, **69**, 723–728.
- Kumar, T. S. V. V., T. N. Krishnamurti, M. Fiorino, and M. Nagata, 2003: Multimodel superensemble forecasting of tropical cyclones in the Pacific. *Mon. Wea. Rev.*, **131**, 574–583.
- Landman, W. A., A. Seth, and S. J. Camargo, 2005: The effect of regional climate model domain choice on the simulation of tropical cyclone—like vortices in the southwestern Indian Ocean. *J. Climate*, **18**, 1263–1274.

- Liu, B., and L. Xie, 2011: A scale-selective data assimilation approach to improving tropical cyclone track and intensity forecasts in a limited-area model: A case study of Hurricane Felix (2007). *Wea. Forecasting*, in press.
- Onogi, K., J. Tsutsui, H. Koide, M. Sakamoto, S. Kobayashi, H. Hatsushika, T. Matsumoto, N. Yamazaki, H. Kamahori, K. Takahashi, S. Kadokura, K. Wada, K. Kato, R. Oyama, T. Ose, N. Manoji, and R. Taira, 2007: The JRA-25 reanalysis. *J. Meteor. Soc. Japan*, **85**, 369–432.
- Pickett, M. H., W. Tang, L. K. Rosenfeld, and C. H. Wash, 2003: QuikSCAT satellite comparisons with nearshore buoy wind data off the U.S. west coast. *J. Atmos. Oceanic Technol.*, **20**, 1869–1879.
- Pielke, R. A., W. R. Cotton, R. L. Walko, C. J. Tremback, W. A. Lyons, L. D. Grasso, M. E. Nicholls, M. D. Moran, D. A. Wesley, T. J. Lee, and J. H. Copeland, 1992: A comprehensive meteorological modeling system-RAMS. *Meteor. Atmos. Phys.*, **49**, 69–91.
- Saito, K., T. Fujita, Y. Yamada, J. Ishida, Y. Kumagai, K. Aranami, S. Ohmori, R. Nagasawa, S. Kumagai, C. Muroi, T. Kato, H. Eito, and Y. Yamazaki, 2006: The operational JMA nonhydrostatic mesoscale model. *Mon. Wea. Rev.*, **134**, 1266–1298.
- Skamarock, W. C., J. B. Klemp, J. Dudhia, D. O. Gill, D. M. Barker, W. Wang, and J. G. Powers, 2005: A description of the advanced research WRF Version 2. *NCAR Technical Note*, NCAR/TN.468+STR.
- Takayabu, I., 2010: An overview presentation on downscaling projects in Japan, paper presented at Workshop on Dynamical Downscaling over Japan. *Int. Comm. on Dynamical Downscaling*, Tsukuba, Japan.
- Von Storch, H., H. Langenberg, and F. Feser, 2000: A spectral nudging technique for dynamical downscaling purposes. *Mon. Wea. Rev.*, **128**, 3664–3673.
- Winterfeldt, J., and R. Weisse, 2009: Assessment of value added for surface marine wind speed obtained from two regional climate models. *Mon. Wea. Rev.*, **137**, 2955–2965.
- Wu, C.-C., R. Zhan, Y. Lu, and Y. Wang, 2012: Internal variability of the dynamically downscaled tropical cyclone activity over the western North Pacific by the IPRC regional climate model. *J. Climate*, in press.
- Zhang, H.-M., J. J. Bates, and R. W. Reynolds, 2006: Assessment of composite global sampling: Sea surface wind speed. *Geophys. Res. Lett.*, **33**, L17714, doi:10.1029/2006GL027086.